

- <sup>1</sup>R. G. Parsons and R. Weinstein, Phys. Rev. Lett. **20**, 1314 (1968); M. Davier, Phys. Lett. **27B**, 27 (1968).  
<sup>2</sup>G. K. Greenhut, R. Weinstein, and R. G. Parsons, Phys. Rev. D **1**, 1308 (1970).  
<sup>3</sup>References to these early experimental papers are given in footnotes 1-4 in Ref. 2.  
<sup>4</sup>*Experimental Meson Spectroscopy*, edited by C. Baltay and A. Rosenfeld (Columbia Univ. Press, New York, 1970).  
<sup>5</sup>A good summary of the data is given by K. Gottfried, in *Proceedings of the 1971 International Symposium on Electron and Photon Interactions at High Energies*, edited by N. B. Mistry (Laboratory of Nuclear Studies, Cornell University, Ithaca, New York, 1972).  
<sup>6</sup>J. Lefrançois, in *Proceedings of the 1971 International Symposium on Electron and Photon Interactions at High Energies*, edited by N. B. Mistry (Ref. 5).  
<sup>7</sup>D. Earles and Y. Srivastava, Northeastern University Report No. NUB 2196 (unpublished).  
<sup>8</sup>P. J. Biggs *et al.*, Phys. Rev. Lett. **24**, 1197 (1970); H. Alvensleben *et al.*, *ibid.* **25**, 1373 (1970); Nucl. Phys. **B25**, 333 (1971).  
<sup>9</sup>P. L. Braccini *et al.*, Nucl. Phys. **B24**, 173 (1970).  
<sup>10</sup>H. J. Behrend *et al.*, Phys. Rev. Lett. **24**, 1246 (1970).  
<sup>11</sup>J. Ballam *et al.*, Phys. Rev. Lett. **24**, 1364 (1970).  
<sup>12</sup>A good summary of the experimental situation in a production from protons is given by G. Wolf, in *Proceedings of the 1971 International Symposium on Electron and Photon Interactions at High Energies*, edited by N. B. Mistry (Ref. 5).  
<sup>13</sup>J. Benecke and H. P. Dürr, Nuovo Cimento **56**, 269 (1968).  
<sup>14</sup>Particle Data Group, Rev. Mod. Phys. **45**, S1 (1973).  
<sup>15</sup>G. K. Greenhut, Phys. Rev. D **2**, 1915 (1970); **3**, 1679(E) (1971).  
<sup>16</sup>A. M. Boyarski *et al.*, Phys. Rev. Lett. **23**, 1343 (1969).  
<sup>17</sup>M. Gell-Mann, D. Sharp, and W. G. Wagner, Phys. Rev. Lett. **8**, 261 (1962).  
<sup>18</sup>We assume that the entire  $\phi \rightarrow 3\pi$  decay occurs via  $\phi \rightarrow \rho\pi$ .  
<sup>19</sup>E. Cremmer and M. Gourdin, Nucl. Phys. **B10**, 179 (1969).  
<sup>20</sup>An early discussion of  $\rho$ - $\omega$  interference in the  $\pi^0\gamma$  state in colliding beams is given by A. Donnachie [Phys. Lett. **27B**, 525 (1968)]. The assumption is made in this paper that the relative phase is  $0^\circ$ .  
<sup>21</sup>Considering the diagrams of Fig. 7 alone does not take into account the unitarization scheme of Ref. 7. The latter may be important in the production of  $\pi^0\gamma$ . In the case dealt with in Refs. 1 and 2, the  $\omega \rightarrow \pi\pi$  branching is rather low and is ignored in colliding-beam production of two pions.  
<sup>22</sup>If the relative colliding-beam phase is  $\beta$ , then the correct  $r_{\omega\rho}$  curve is obtained from the solid curve in Fig. 8 by renormalizing it to unity at  $\Delta_\omega - \Delta_\rho = \beta$ .  
<sup>23</sup>J. D. Jackson, Nuovo Cimento **34**, 1644 (1964).  
<sup>24</sup>If the vector-meson photoproduction amplitudes are written

$$\frac{d\sigma}{dt} = \left( \frac{em_V^2}{2\gamma_V} \right)^2 a_V e^{b_V t},$$

then  $b_\rho \approx b_\omega \approx b_\phi$  and  $a_\rho \approx a_\omega$ , but  $a_\phi \approx \frac{1}{17} a_\rho$ .  
<sup>25</sup>The equivalent curves for the  $\rho$ - $\omega$  case would overlap.

### Deck-model calculation of $\pi^- p \rightarrow \pi^- \pi^+ \pi^- p$ †,‡

G. Ascoli, R. Cutler, L. M. Jones, U. Kruse, T. Roberts, B. Weinstein, and H. W. Wyld, Jr.

Physics Department, University of Illinois at Urbana-Champaign, Urbana, Illinois 61801

(Received 26 November 1973)

We formulate and study a Deck-type model for the reaction  $\pi^- p \rightarrow \pi^- \pi^+ \pi^- p$ . The model differs from previous Deck calculations in two respects: (i) Experimental data are used for both  $\pi\pi$  and  $\pi N$  scattering, and (ii) the amplitude has proper Bose symmetry. Feature (i) allows us to examine any desired region of  $3\pi$  mass (the  $A_3$  is treated on the same footing as the  $A_1$ ); features (i) and (ii) allow us to examine all the angular dependence in the final state and to compare with partial-wave analyses of experimental data. In this paper we present the results of a study in which events generated from the model by a Monte Carlo method are plotted and fitted in the same way as experimental events. Many of the features of the data are qualitatively reproduced, including certain important properties obtained from the partial-wave analysis in the  $A_1$  region. The  $A_3$  region is not accurately represented by the model. Results of an analytic partial-wave analysis of this model, and the use of it to check the assumptions of the fitting program, are presented in an associated paper.

#### I. INTRODUCTION

Recent analyses of the world's data on the reaction  $\pi^- p \rightarrow \pi^- \pi^+ \pi^- p$  in the  $A_1$  (see Ref. 1) and  $A_3$  (see Ref. 2) regions have led to some puzzling results. The  $A_1$  effect may be isolated as a resonance-

like bump in the  $\rho\pi L=0$  ( $J^P=1^+$ ) partial wave, and the  $A_3$  effect may be isolated as a similar bump in the  $f\pi L=0$  ( $J^P=2^-$ ) partial wave. However, when the phase of these amplitudes relative to other (more smoothly behaving) amplitudes is determined in the region near the bump, no evidence

of rapid variation is seen. In other words, the mass spectrum looks like a resonance but the phase shift does not have typical Breit-Wigner variation.

Over the past several years, a number of calculations have been done using Reggeized Deck models.<sup>3</sup> These models, usually of the reaction  $\pi^- N \rightarrow \pi^- \rho^0 N$ , provide a nice bump at approximately the  $A_1$  position without any resonance pole at all. Although the shape of the bump is not exactly the same as the experimentally observed  $A_1$ , and the total  $A_1$  production cross section calculated by this method tends to be too small by a factor of about 2, the model has many physically attractive features.

We decided to extend the model so that it explicitly describes  $\pi^- p \rightarrow \pi^- \pi^+ \pi^- p$  without the requirement that one  $\pi^+ \pi^-$  pair be in the  $\rho$  and with the requirement that the amplitude be symmetrized in the two identical  $\pi^-$  particles. The aim of the study was to have a model for all the angular dependence in the 4-body final state; this would allow us to examine partial waves of the three-pion system and to compare these with experimental results. Since we do not restrict ourselves to  $M_{\pi^+ \pi^-} = m_\rho$ , we can examine regions outside the  $A_1$  peak; in particular we can include the  $A_3$ , for which  $M_{\pi^+ \pi^-} \approx m_f$ .

In Fig. 1, we display the amplitudes taken into consideration. Our net amplitude is a sum of terms. Each term is a product of a pion-pion scattering amplitude, a pion propagator, and a pion-nucleon scattering amplitude. Both the  $\pi^+ \pi^-$  and the  $\pi^- \pi^-$  scattering are included. The  $\pi\pi$  and  $\pi N$  scattering amplitudes used are for *on-shell* pions; no attempt has been made to continue amplitudes off shell in the mass. This greatly reduces the number of variable parameters. We have adopted this on-shell philosophy because we feel that the theoretical uncertainties involved in off-shell extrapolations are as great as the theoretical uncertainties in using the Deck model to begin with. We wish to make the model as straightforward as possible. One could probably improve agreement with the data if a different off-shell extrapolation form factor was used for each partial wave; however, we cannot get excited about this procedure and will not discuss it further.

The amplitudes used for the  $\pi\pi$  and  $\pi N$  scattering were the best available to us at the time. We examined results for various Reggeized and un-

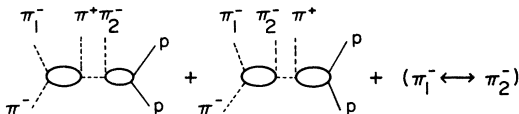


FIG. 1. Our Deck model for  $\pi^- p \rightarrow \pi^- \pi^+ \pi^- p$ .

Reggeized versions of the pion propagator. These components of the model are discussed in detail in Sec. II.

Monte Carlo generation was used to obtain a sampling of several thousand events in the region  $0.9 \text{ GeV} \leq M_{3\pi} \leq 1.8 \text{ GeV}$  for each version of the pion propagator considered. The three-pion mass spectra for different versions were compared with the data at 16 GeV/c incident laboratory pion momentum. After a "best" Reggeized propagator was decided upon, another set of events was generated at 40 GeV/c; this gives us some indication of the energy dependence of the results. A standard SUMX program was used to compile distributions in various angles and invariant masses. These are discussed and compared with the data in Sec. III.

Next, the events obtained from our formula were fitted by the same fitting program used by Ascoli *et al.* in the data analysis which motivated this work.<sup>1,2</sup> This yielded relative amounts of the various partial waves present, and their phases. These are compared with the data in Sec. IV. Qualitative agreement is obtained in many cases. Furthermore, some phase relations in the data which seem perplexing at first can be understood by examining the phases produced by models of progressively increasing complexity. Generally speaking, the model reproduces the  $A_1$  region quite well but fails to provide a large enough  $A_3$  effect.

The isospin dependence of the model was checked by predicting  $\pi^- n \rightarrow \pi^- \pi^- \pi^0 p$  at 7 GeV/c and comparing with published data. There is good agreement in this case also. Encouraged by these successes, we have used the model to predict a cross section for  $A_1$  production for energies up to  $P_{\text{lab}} = 640 \text{ GeV/c}$ . These results are presented and discussed in Sec. V.

Finally, Sec. VI is devoted to some comments by way of summary.

## II. COMPONENT PIECES OF THE MODEL

### A. Amplitudes for pion-pion scattering

Experimental information on pion-pion scattering is available up to  $m_{\pi\pi} = 3.0 \text{ GeV}$ , and phase shifts and elasticities are available in one form or another up to  $m_{\pi\pi} = 1.48 \text{ GeV}$ . At the time we began this calculation, the best  $\pi^+ \pi^-$  phase shifts available in the  $\rho$  region were those of Protopopescu *et al.*<sup>4</sup>; since our description of angular dependence in the  $A_1$  region depends crucially on the  $\pi^+ \pi^-$  parameterization near the  $\rho$  we used the Protopopescu phase shifts and elasticities in the region  $0.55 \text{ GeV} \leq M_{\pi\pi} \leq 1.15 \text{ GeV}$ . It should be noted that the  $\pi^- \pi^-$  phase shifts used by this group to extract their isospin-zero phase shifts were those of Baton *et al.*<sup>5</sup>

Phase shifts for the region of  $\pi\pi$  energy below

550 MeV are all relatively small. These were obtained by extrapolation of the Protopopescu phase shifts and reference to the work of Walker *et al.*,<sup>6</sup> Lovelace, Heinz, and Donnachie,<sup>7</sup> and Scharen-guivel *et al.*<sup>8</sup> In the region  $1.0 \text{ GeV} \leq M_{\pi\pi} \leq 1.48 \text{ GeV}$ , phase shifts and elasticities have been given by Oh *et al.*<sup>9</sup> and the CERN-Munich collaboration.<sup>10</sup> We matched these onto the Protopopescu phase shifts. This procedure gave us a smooth set of phase shifts and elasticities covering the region from threshold to 1.48 GeV; the bulk of the information is from Protopopescu *et al.* and most of our results in the  $A_1$  region depend essentially totally on the Protopopescu results.

In order to obtain a description of  $\pi\pi$  scattering for higher  $\pi\pi$  energies, we are forced to use a model. Since the highest  $3\pi$  mass considered is 1.8 GeV, the largest  $\pi\pi$  energy of concern is 1.66 GeV. Hence the region not covered by explicit phase-shift analyses is fairly small. The only feature of note in this region is the  $g$  resonance. We therefore approximated the invariant  $\pi\pi$  scattering amplitude in the region above 1.48 GeV by computing the amplitude from the phase shifts at 1.48 GeV and adding to this a Breit-Wigner distribution for the  $g$ .

### B. Amplitudes for pion-nucleon scattering

Experimental information on  $\pi N$  scattering is available over a full range of energies. Again, we use a phase-shift parameterization for the lower energies, choosing the CERN 1967 solution.<sup>11</sup> These phase shifts extend down through the  $\Delta_{33}$  resonance region.

For the higher energies ( $M_{\pi N} \geq 1.96 \text{ GeV}$ ) we have used the Regge-pole fit of Barger and Phillips.<sup>12</sup> For our purposes, this fit has the advantage that finite-energy sum rules utilizing low-energy data were used in addition to fits to the high-energy data to determine the Regge residues. Thus some degree of continuity between the two regions has been ensured.

Unfortunately the phase-shift and Regge parameterizations do not match exactly at 2 GeV. In figures 2(a) and 2(b) we show the  $\mathcal{G}$  and  $\mathcal{B}$  invariant amplitudes for  $\pi N$  scattering as calculated from phase shifts and from the Regge parameterization, at  $t=0$ . There is a marked discontinuity between the two formulas, especially in the  $\mathcal{G}$  amplitude. The particular combination,  $\mathcal{C}$ , of  $\mathcal{G}$  and  $\mathcal{B}$  which occurs in the direct-channel helicity-conserving amplitude is plotted in Fig. 2(c). Note that this amplitude has a smaller discontinuity.

We have arbitrarily smoothed over the "join" between the two approximations by making a linear interpolation at each  $\cos\theta$  value between the

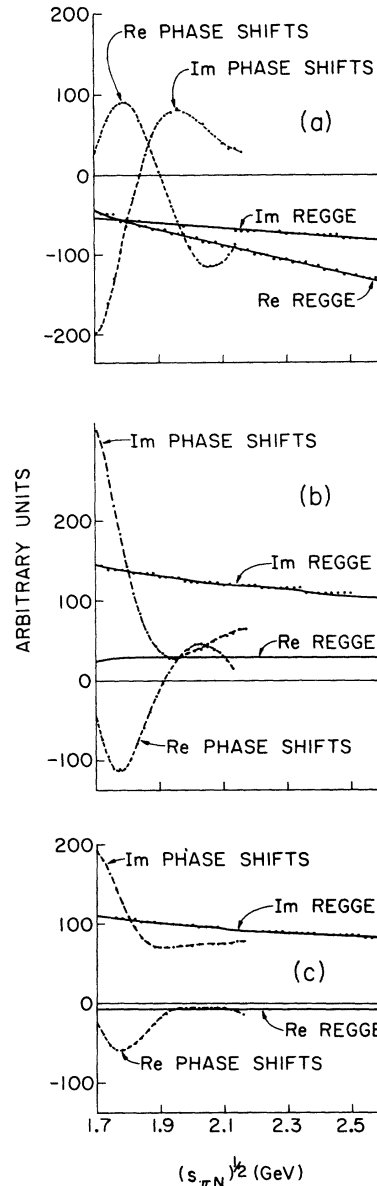


FIG. 2.  $\pi^-$ -proton elastic scattering amplitudes at  $t=0$  calculated from Regge formulas and from phase shifts, in the transition region. (a) The invariant amplitude  $\mathcal{G}$ ; (b) the invariant amplitude  $\mathcal{B}$ ; (c) the  $s$ -channel helicity-conserving amplitude  $\mathcal{C}$ .

phase-shift approximation at  $(s_{\pi N})^{1/2} = 2 \text{ GeV}$  and the Regge approximation at  $(s_{\pi N})^{1/2} = 2.2 \text{ GeV}$ . This is a reasonable approach because the dominant amplitude in our calculation actually depends chiefly on  $\mathcal{C}$ , at large energies for the incident pion.<sup>13</sup>

### C. Pion propagator

Deck, in his original formulation of the model,<sup>14</sup> emphasized that in the center-of-mass system one

expects a forward-moving  $\rho\pi$  system because of the diffractive nature of  $\pi N$  scattering, and a forward-moving  $\rho$  because of the pion propagator. Thus the probability that the  $\pi$  also travels forward, keeping  $s_{\rho\pi}$  near threshold, is enhanced over phase space. Berger<sup>3</sup> was able to sharpen the peak near threshold by Reggeizing the amplitude. Crudely speaking, this sharpening of the peak is produced because a factor like  $s_{\rho\pi}^{\alpha_{\pi}(t)}$  will damp at large  $s_{\rho\pi}$  [ $\alpha_{\pi}(t)$  is negative for all  $t$  in the scattering region]. In addition to these basic components of the pion Regge propagator, we have allowed for a Regge residue function of exponential form  $e^{at}$ . The parameter  $a$  is the only free parameter in our model.

We have studied "pure" Deck amplitudes with propagator of the form

$$\frac{e^{at}}{t - m_{\pi}^2} \quad (2.1)$$

and "Reggeized" Deck amplitudes with propagator of the form

$$\frac{(\text{appropriate mass})^{\alpha_{\pi}(t)} e^{-t\pi\alpha_{\pi}(t)/2} e^{at}}{t - m_{\pi}^2} \quad (2.2)$$

However, the choice of the "appropriate mass" in Eq. (2.2) is much less clear in our model than in Berger's, and some discussion of this point is in order.

In a model like Berger's (see Fig. 3), Reggeization of the pion exchange clearly calls for a term of the form  $s_{\rho\pi}^{\alpha_{\pi}(t)}$  in the region where  $s_{\rho\pi}$  is much larger than some reference  $(\text{mass})^2$ ,  $s_0$ , generally estimated to be near  $1 \text{ GeV}^2$ . Since the  $A_1$  itself has a mass of only  $1.08 \text{ GeV}$ , the asymptotic formula need not apply near the  $A_1$  bump. In an attempt to extend the Regge idea to this nonasymptotic region, Berger replaced  $s_{\rho\pi}$  by  $2q_t k_t \cos\theta_t$  for the internal reaction  $\pi + \text{"Pomeron"} \rightarrow \pi + \rho$  (here "Pomeron" stands for the dynamical mechanism carrying momentum  $p_{\text{nuc}}^{\text{in}} - p_{\text{nuc}}^{\text{out}}$ ). If  $u_{\rho\pi}$  and  $t_{\rho\pi}$  are momentum transfers for this internal reaction, Berger's attempt replaces  $s_{\rho\pi}$  by

$$\frac{s_{\rho\pi} - u_{\rho\pi}}{2} + \frac{(m_{\rho}^2 - m_{\pi}^2)(m_{\pi}^2 - t)}{2t_{\rho\pi}}.$$

This replacement further enhances the peak over a simple  $s_{\rho\pi}$  factor.

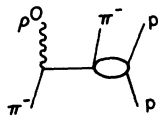


FIG. 3. Berger's Deck model for  $\pi^- p \rightarrow \rho^0 \pi^- p$ .

Unfortunately, Berger's formula is singular at  $t_{\rho\pi} = 0$ , and we now know that such singular terms are canceled by daughter trajectories. A more modern version of this recipe for fixing up Regge formulas in nonasymptotic regions would therefore be to replace  $s_{\rho\pi}$  by  $\frac{1}{2}(s_{\rho\pi} - u_{\rho\pi})$ . Hence we drop the term proportional to  $1/t_{\rho\pi}$  in  $2q_t k_t \cos\theta_t$ . This will produce an  $A_1$  bump more pronounced than  $s_{\rho\pi}^{\alpha_{\pi}(t_{\rho\pi})}$  alone, but less pronounced than the result of Berger.

Recipes of this sort for Reggeizing nonasymptotic regions are more of an art than a science. Duality tells us that Regge formulas (no matter how they are "fudged") can only approximate low-energy behavior; certainly resonances like the  $A_2$  are important in the  $\pi^- \pi^+ \pi^-$  state, and these cannot be reproduced by Regge formulas. However, if we accept these limitations, there are several indications in recent Regge fits to other reactions that the replacement of  $s^\alpha$  by  $[\frac{1}{2}(s-u)]^\alpha$  improves the fit for low  $s$ .<sup>15</sup>

Therefore, if we produced a  $\rho\pi$  system, our plan of attack would be relatively clear. However, in our amplitude, where three individual pions are produced, one can imagine four different ways to Reggeize each term in the amplitude. These are pictured in Fig. 4, and the choice of the correct one is determined by the particular values of the subenergies being considered.

(i) Figure 4(a) represents a situation in which  $s_{12}$ ,  $s_{23}$ ,  $s_{34}$  are all large. In this case the factor appropriate to the pion propagator would be  $s_{23}^{\alpha_{\pi}(t)}$ .

(ii) Figure 4(b) represents a situation in which  $s_{12}$  is at a resonance, but  $s_{123}$  and  $s_{34}$  are large. This is the Berger picture. The correct factor here is  $s_{123}^{\alpha_{\pi}(t)}$ .

(iii) Figure 4(c) represents a situation in which

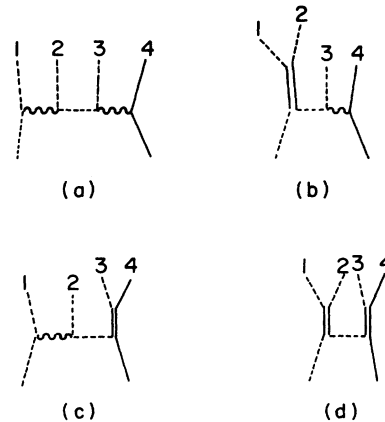


FIG. 4. Kinematic regions of interest in the final state of  $\pi^- p \rightarrow \pi^- \pi^+ \pi^- p$ . (a) Triple-Regge region; (b) dipion resonance; (c)  $\pi N$  resonance; (d) double-resonance production.

$s_{34}$  is in a resonance region, but  $s_{12}$  and  $s_{234}$  are large. This is the situation considered by Jones<sup>16</sup> in studying the nucleon- $\pi$ - $\pi$  enhancement in this reaction. The correct factor here is  $s_{234}^{\alpha_\pi(t)}$ .

(iv) Figure 4(d) represents the case where  $s_{12}$  and  $s_{34}$  are both in the resonance region, but  $s$  is large. The correct factor here is  $s^{\alpha_\pi(t)}$ .

Since we have included all the  $\pi$ -nucleon scattering amplitudes, with resonances at the lower energies, we have the possibility that each of the four forms may be valid at some time in the calculation. This raises the spectre of "Balkanization" of the allowed phase space into regions where one or the other of the forms is applicable. There are many practical reasons to avoid such a division if possible. Hence we decided to settle on a form that is "correct" for most of the events in the region we wish to study.

Limiting the three-pion mass to  $0.9 < M_{3\pi} < 1.8$  GeV at an incident energy of 16 GeV/c allows  $s_{\pi N}$  to range from values near threshold to 25 GeV<sup>2</sup>. Most of our events will have  $s_{\pi N}$  larger than 4 GeV<sup>2</sup>. We therefore eliminate from consideration the formulas attached to Figs. 4(c) and 4(d).

Furthermore, we can see that events of the type represented Fig. 4(a) will be rare. This is because  $s_{12} + s_{23} + s_{13} = M_{3\pi}^2 + 3M_\pi^2$ , and if  $m_{3\pi} \sim 1.1$  GeV each of the individual  $s_{ij}$  must be below  $(1.1)^2$ . In a typical event,  $s_{23}$  will be around 0.4 or 0.5 GeV<sup>2</sup>. Hence Reggeizing the pion propagator with a factor of  $s_{23}^{\alpha_\pi(t)}$  will raise even worse problems of non-asymptoticity than Reggeizing the situation in Fig. 4(b) by  $s_{123}^{\alpha_\pi(t)}$ .

We conclude that a Reggeized propagator with energy dependence of the form  $s_{3\pi}^{\alpha_\pi(t)}$  will be our best choice for the kinematic region considered. We may hope to improve this at low values of  $s_{3\pi}$  by using

$$\left[ s_{123} + \frac{1}{2}(t_{\pi(12)}) - \frac{1}{2}t_{NN} - M_\pi^2 - \frac{1}{2}s_{12} \right]^{\alpha_\pi(t)} \equiv \left[ \frac{1}{2}(s_{3\pi} - u_{3\pi}) \right]^{\alpha_\pi(t)}.$$

This reduces to Berger's formula (less his singularity) when  $s_{12} = m_\rho^2$ .

In the discussion below of model calculations the propagators used are associated with acronyms for their composition. We list here a glossary of these terms.

$$\text{PDK: } \frac{e^{at}}{t - m_\pi^2}, \quad (2.3)$$

$$\text{FULL: } \frac{s_{3\pi}^{\alpha_\pi(t)} e^{at} e^{-i\pi\alpha_\pi(t)/2}}{t - m_\pi^2}, \quad (2.4)$$

$$\text{SMU: } \frac{\left[ \frac{1}{2}(s_{3\pi} - u_{3\pi}) \right]^{\alpha_\pi(t)} e^{at} e^{-i\pi\alpha_\pi(t)/2}}{t - m_\pi^2}. \quad (2.5)$$

### III. CALCULATED DISTRIBUTIONS

#### A. Distribution in the three-pion mass

The first distribution compared with the data in studies of this sort is, of course, the three-pion mass spectrum. In Fig. 5 we show, for reference, an experimental spectrum obtained by combining the world's data in the interval  $11 \text{ GeV}/c \leq P_{\text{lab}} \leq 25 \text{ GeV}/c$ .<sup>17</sup> This shows the  $A_2$  and  $A_3$  peaks more clearly than the data at any one energy.

One of the main selling points for Berger's Reggeization of the Deck model was its sharpening of the lump in the  $A_1$  region; we would therefore expect FULL and SMU to produce more sharply defined peaks than PDK. In Fig. 5 we show the calculation from our "best" SMU (with  $a=0$ ). Notice that both the normalization and the over-all shape of the spectrum are reproduced rather well, except in the  $A_2$  region. Our best PDK results, with  $a=2$ , are displayed in Fig. 6(a). They are, as expected, quite a bit flatter than the predictions of the Reggeized SMU. We were unable to make the  $A_1$  in PDK any more pronounced, within the constraints of this model.

If we scrutinize the results more critically, we realize that even the  $A_1$  enhancement produced by SMU is rather wider than might be desired, since some of the experimental events in the broad hump at low  $3\pi$  masses must surely be contributed by the tail of the  $A_2$ . In fact, all of our calculations in this model have produced peaks which were a little wider than we might have expected from Berger's result. After some experimentation, we have come to the conclusion that this difference is essentially due to the fact that our calculation, with all  $\pi\pi$  waves included, fills up more of the

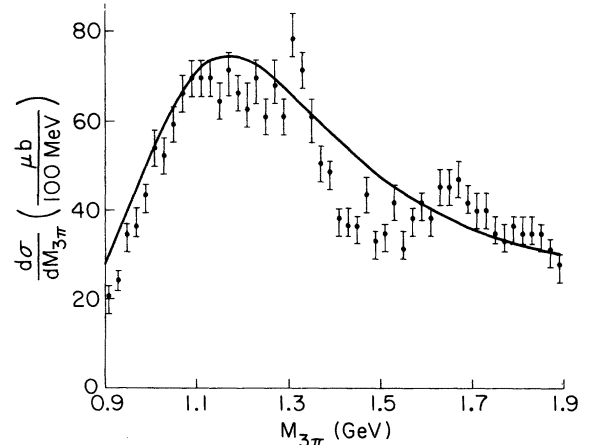


FIG. 5.  $3\pi$  mass distribution. The data points are combined 11–25 GeV/c data; the curve is calculated from our Deck model. Asymmetric errors are due to "quantization" of computer plotting routine.

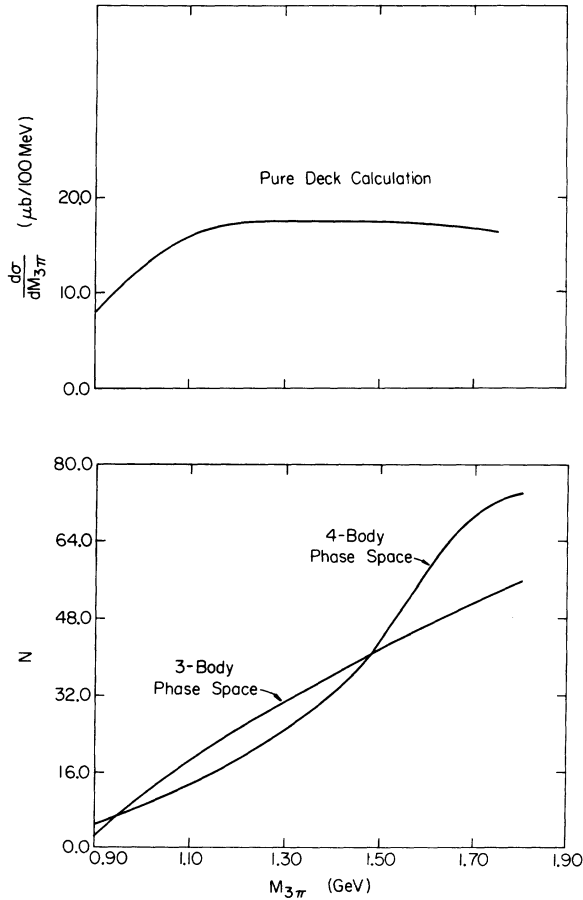


FIG. 6. (a) Deck calculation with elementary pion propagator. (b) Shapes of  $\rho\pi p$  and  $\pi\pi p$  phase space.

available 4-body phase space than Berger's (which is essentially a 3-body calculation).

Berger uses three-particle  $\rho\pi p$  phase space. It rises very sharply from the  $\rho\pi$  threshold to about the  $A_1$  peak, and then rises more slowly as  $m_{3\pi}$  is increased. The four-body  $\pi\pi p$  phase space used in our calculation rises from the  $3\pi$  threshold and grows rapidly for  $3\pi$  masses just above the  $A_1$  [see Fig. 6(b)]. Hence our amplitude would have to fall very rapidly as a function of three-pion mass to provide a sharp  $A_1$  peak. The Regge  $(s_{123}-u_{123})^{\alpha_\pi}$  factor apparently is just not adequate for this purpose.

Another difference between the data and our model is the absence of an  $A_3$  bump in our mass spectrum. As is demonstrated in I, there is an  $A_3$  present in the  $f_\pi$   $s$ -wave  $2^-$  state, but it is obscured by the many other partial waves of equal size predicted by the model.<sup>18</sup> We found that SMU tended to produce slightly more  $f^0$  particles than did FULL, and so made the  $A_3$  effect as large as possible. For this reason, we selected SMU as our

"best" amplitude. All the rest of the results discussed in this section were calculated using SMU.

Calculations with FULL and SMU for various values of the parameter  $a$  in Eq. (2.5) showed that reasonable shapes for the  $3\pi$  mass spectra could only be obtained with positive  $a$  less than 1 or 2. A small value of  $a$  is also expected from the slope of the differential cross section for  $\pi N \rightarrow \rho\Delta$ . For SMU we found that  $a=0$  worked very well; this reduces the model to its simplest possible form. All results discussed below are for this value of  $a$ .

### B. Overview of other distributions

The phase space for our reaction  $\pi N \rightarrow \pi\pi\pi N$  at fixed incident energy can be written as

$$\frac{2\pi}{8\sqrt{s}p_{in}} d\alpha d\cos\beta d\gamma ds_{12} ds_{23} dt_{NN} \frac{dM_{3\pi}}{M_{3\pi}}.$$

Here  $t_{NN}$  is the momentum transfer between the nucleons,  $s_{12}$  and  $s_{23}$  are Dalitz-plot variables for the three pions in their over-all rest frame, and  $\alpha$ ,  $\beta$ , and  $\gamma$  are a set of Euler angles describing the orientation of the three pions in this system. In this paper we take  $\alpha$  and  $\beta$  to be the polar angles of the  $\pi^+$ , with  $\beta$  being the angle between the  $\pi^+$  and the incident  $\pi^-$  direction. The third angle,  $\gamma$ , is the angle between the  $3\pi$  decay plane and the plane formed by the direction of the incident  $\pi^-$  and the outgoing  $\pi^+$ .

We can therefore study single distributions in  $\alpha$ ,  $\cos\beta$ ,  $\gamma$ ,  $s_{12}$ ,  $s_{23}$ , and  $t_{NN}$  as well as  $M_{3\pi}$ . Furthermore, we can study the  $M_{3\pi}$  dependence of each of these distributions by collecting events in narrow  $M_{3\pi}$  bins. This allows us to isolate behavior in the  $A_1$  region from that in the  $A_3$  region. Finally, we can examine distributions in other variables, such as  $s_{\pi^+\pi^-}$ ,  $s_{\pi^+\pi^-}$ , etc. By comparing all these distributions with the data, we can get a very good over-all picture of the strengths and weaknesses of our model.

It is clearly impossible to show histograms of all these distributions. In order to summarize our results as efficiently as possible, we have organized this information into three parts presented below as Secs. III C, III D, and III E. In Sec. III C we describe the distributions in  $\alpha$ ,  $\gamma$ , and  $t_{NN}$ , as well as the energy dependence of the various distributions. These features are fairly straightforward and can be summarized primarily in words. Section III D is devoted to the distributions in  $\cos\beta$ ,  $s_{\pi^+\pi^-}$ ,  $s_{\pi^-\pi^-}$ , and the  $\pi\pi$  scattering angles. Variation of these distributions with  $M_{3\pi}^2$  is an important feature of the data, and the extent to which our model reproduces this is a good test of the model. We note in passing that only models like ours, with all partial waves of  $\pi\pi$  scattering included, can hope to predict mass dependence of the  $\alpha$ ,  $\beta$ , and  $\gamma$  distributions. Hence this is a new feature of our

calculation, and we feel justified in devoting a fair amount of space to it. Finally, Sec. III E describes the distributions in pion-nucleon and  $\pi$ - $\pi$ -nucleon mass; we find that the agreement with data is also reasonably good for these distributions.

### C. Some distributions with simple behavior

Both in the data and in the model, distribution of events in the Euler angle  $\alpha$  is quite flat. This is independent of energy and of three-pion mass.

The Euler angle  $\gamma$  has more interesting behavior. Due to parity and the identity of the negative pions, the projection on  $\gamma$  is forced to be symmetric about  $\gamma=0$  and  $\gamma=\pi/2$ . In general, it has structure, with a peak at  $\gamma=0$  and a dip at  $\gamma=\pi/2$ ; the peak grows more pronounced as  $M_{3\pi}^2$  increases. This is true in both the data and the model.

Over-all  $t_{NN}$  dependence is governed largely by the behavior of the  $\pi N$  scattering amplitude inserted. At large  $s_{\pi N}$  this is like  $e^{4t_{NN}}$ ; hence we expect the calculated cross section to behave roughly like  $e^{8t_{NN}}$ . This is borne out in practice: At 16 GeV/c incident pion energy, the calculated distribution in  $t_{NN}$  for all our events in the region  $0.9 \text{ GeV} \leq M_{3\pi} \leq 1.8 \text{ GeV}$  is an exponential of slope  $8.8 \pm 1.5$ ; this compares with a slope for the experimental distribution at 16 GeV of  $8.3 \pm 0.4$ . The calculated slope gradually decreases as the three-pion mass increases. This compares well with the behavior of the experimental distributions.

The distribution of events in other momentum transfers has also been studied. The momentum transfer between the incident pion and the outgoing  $\pi^- \pi^+$  pair, where the  $\pi^-$  is chosen to be that one forming a resonance with the  $\pi^+$ , is the variable associated with our pion-exchange propagator. If the model is a reasonable approximation to reality, distributions in this momentum transfer should be similar to (or perhaps sharper than) the data. In Fig. 7, we show some of these distributions. The momentum transfer to the  $\rho$  in the  $A_1$  region is quite well reproduced by the model. In the  $A_3$  region, the model predicts somewhat sharper distributions in momentum transfer to the  $\rho$  and  $f$  than are observed in the experiment.

The calculated three-pion mass distributions (not shown) at 40 GeV/c look remarkably similar to those at 16 GeV/c; in particular the production of  $f^0$  is similar. Gross shapes of  $N\pi$  and  $N\pi\pi$  spectra are affected principally by the kinematic cut-offs; hence the positions of the broad peaks in some of these spectra move up as the energy increases. The energy dependence of the total cross section for events in the mass region  $1.05 \text{ GeV} \leq M_{3\pi} \leq 1.25 \text{ GeV}$  is described in Sec. V.

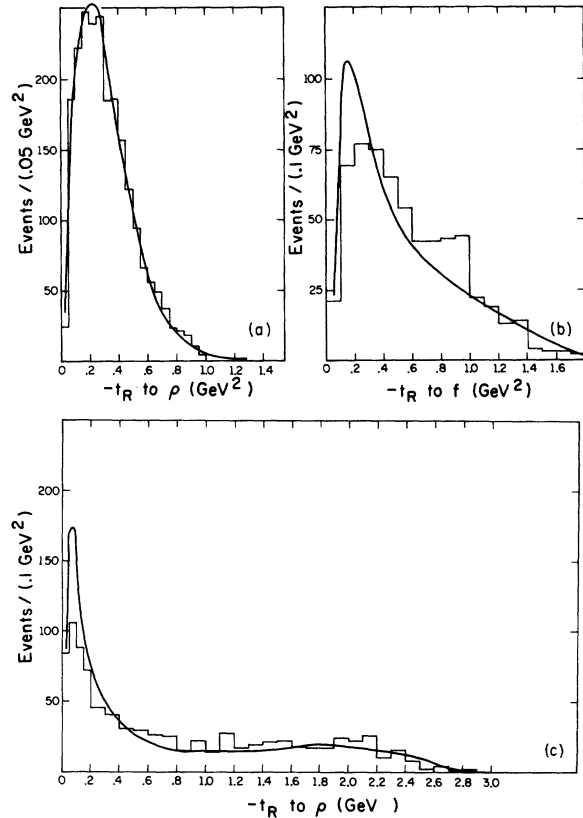


FIG. 7. Distributions in  $t_{\text{Regge}}$ . Histogram shows 11–25 GeV data; curve shows calculation. (a) Momentum transfer to  $\rho$ , for  $1.0 \text{ GeV} \leq M_{3\pi} \leq 1.1 \text{ GeV}$ . Both curves are normalized to 2193 events. (b) Momentum transfer to  $f$ , for  $1.5 \text{ GeV} \leq M_{3\pi} \leq 1.8 \text{ GeV}$ . Both curves are normalized to 612 events. (c) Momentum transfer to  $\rho$ , for  $1.5 \text{ GeV} \leq M_{3\pi} \leq 1.8 \text{ GeV}$ . Both curves are normalized to 694 events.

### D. Distributions closely related to $\pi\pi$ scattering

We expect the distribution in  $M_{\pi^+\pi^-}$  to display bumps corresponding to all  $\pi^+\pi^-$  resonances that are kinematically allowed. In practice, this means only the  $\rho$  in the  $A_1$  region ( $0.9 \text{ GeV} \leq M_{3\pi} \leq 1.2 \text{ GeV}$ ), and both the  $\rho$  and the  $f$  in the  $A_3$  region ( $1.5 \text{ GeV} \leq M_{3\pi} \leq 1.8 \text{ GeV}$ ). Our results at 16 GeV/c are displayed in Fig. 8, where we have normalized our distributions to the data to make comparison of the details easier (due to the approximate correctness of our predicted over-all normalization, as shown in Fig. 5, this is not much of a “cheat”).

Notice that our  $f$  bump is not as prominent, relative to the  $\rho$ , as it is in the data. Since our input  $\pi\pi$  scattering amplitudes come up to the unitarity limit at the  $f$ , we cannot increase the amount of  $f$  in any simple way within this model. Clearly the lack of prominence of the  $f$  is related to the invisibility of the  $A_3$  in our mass spectrum.

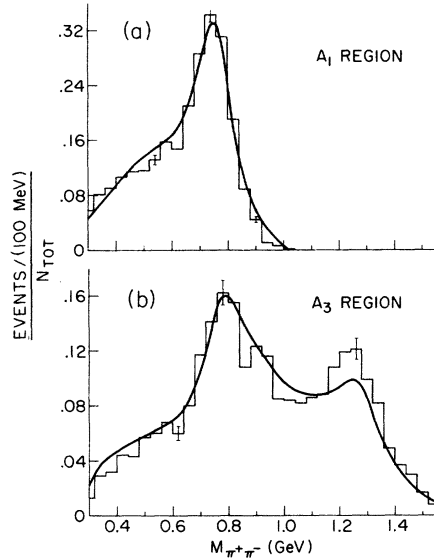


FIG. 8. Distributions in  $M_{\pi^+\pi^-}$ : (a) in  $A_1$  region; (b) in  $A_3$  region.

Another distribution closely related to this is the one in  $\cos\beta$ . The angle  $\beta$  is defined as the angle between the outgoing  $\pi^+$  and the incident  $\pi^-$  in the over-all rest frame of the  $3\pi$  system. When  $M_{3\pi}$  is near threshold for a quasi-two-body  $(\pi^+\pi^-)_R\pi^-$  channel, the  $(\pi^+\pi^-)_R$  system is almost at rest also. In this case, the angle  $\beta$  approximates the angle between the incident  $\pi^-$  and outgoing  $\pi^+$  in the center-of-mass frame of  $\pi^+\pi^-$  scattering. Hence  $\pi-\beta$  is close to  $\theta_{\pi\pi}$ , the  $\pi\pi$  scattering angle. Thus we see that the approximation  $\cos\beta \approx -\cos\theta_{\pi\pi}$  is valid near the  $\rho\pi$  threshold and near the  $f\pi$  threshold; this should aid us in understanding the  $A_1$  and  $A_3$  regions.

We divide our events into three regions in  $M_{3\pi}$ : (i) the  $A_1$  region,  $0.9 \text{ GeV} \leq M_{3\pi} \leq 1.2 \text{ GeV}$ , (ii) the  $A_2$  region,  $1.2 \text{ GeV} \leq M_{3\pi} \leq 1.5 \text{ GeV}$ , and (iii) the  $A_3$  region,  $1.5 \text{ GeV} \leq M_{3\pi} \leq 1.8 \text{ GeV}$ . Calculated distributions in  $\cos\beta$  for these three regions are shown as solid lines in Fig. 9. We note a steady progression from one region to another; the originally broad peak near  $\cos\beta = -1$  becomes narrower as  $M_{3\pi}$  increases and the number of events near  $\cos\beta = +1$  builds up in compensation.

The  $A_2$  region is not directly comparable with the data, as the Deck model produces no  $A_2$ . Experimental distributions for the  $A_1$  and  $A_3$  regions are shown as histograms in Figs. 9(a) and 9(c). We see that our model reproduces qualitatively the data in the  $A_1$  region, but it has more asymmetry than the data. This is related to the large amount of  $0^- \epsilon\pi$  ( $s$  wave) produced by the model, discussed further below. In addition the depletion near  $\cos\beta = -1$  does not proceed fast enough as  $M_{3\pi}$  in-

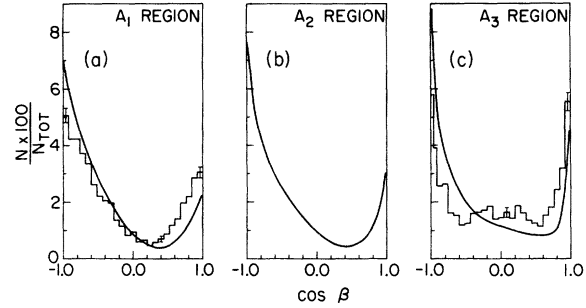


FIG. 9. Distributions in  $\cos\beta$ , where  $\beta$  is the angle between the incident  $\pi^-$  beam and the outgoing  $\pi^+$  particle in the  $3\pi$  center-of-mass system.

creases. The experimental events in the  $A_3$  region are concentrated near  $\cos\beta = +1$  to a greater extent than are the calculated ones.

We can use our quasi-two-body threshold approximation to attempt an interpretation of this behavior. In the  $A_1$  region, the peaking near  $\cos\beta = -1$  represents a peaking of the  $\pi\pi$  differential cross section near  $\cos\theta_{\pi\pi} = +1$ , and the shape of the curve shows clearly a  $\rho-\epsilon$  interference. This is well reproduced by our model.

In the  $A_3$  region, the data show fairly clearly the angular dependence of a spin-2 object interfering with spin 0 and possibly spin 1. Our calculation shows this less well. More light will be cast on this problem in Sec. IV, where we demonstrate that calculated " $f\pi$  in  $s$  wave near threshold" is not larger than " $\rho\pi$  in  $p$  wave away from threshold" in this  $A_3$  region. This is rather different from the experimental result, and may be pinpointed as the cause of all the differences discussed so far.

The  $\pi^-\pi^-$  distributions are expected to be smooth, as no resonances occur in this system. These distributions are shown in Fig. 10. We see that the data are reproduced fairly well.

#### E. Mass distributions involving nucleons

Since our model contains a fairly detailed description of pion-nucleon scattering we might hope for a good match between the predicted and measured  $\pi N$  and  $\pi\pi N$  distributions. This expectation is confirmed qualitatively, although not all details match up exactly.

In Figs. 11 and 12 we compare the calculated and experimental  $p\pi^+$  and  $p\pi^-$  mass distributions. Only events with  $M_{3\pi}$  in the  $A_1$  or the  $A_3$  region are shown; the presence of an  $A_2$  resonance in the data influences the experimental  $\pi N$  spectra for  $M_{3\pi}$  near the resonance. Note that the  $\pi N$  resonance production is more or less correctly reproduced. The general shape of the spectra at  $s_{\pi N}$  larger than shown in Figs. 11 and 12 also agrees with the data

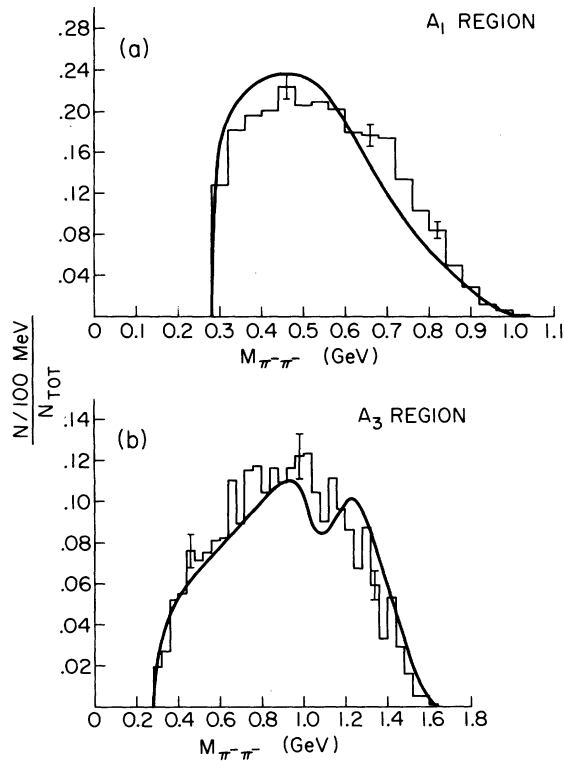


FIG. 10. Distributions in  $M_{\pi^-\pi^-}$ : (a) in  $A_1$  region; (b) in  $A_3$  region.

in that the  $p\pi^+$  distribution falls off more rapidly at large  $M_{p\pi}$  than does the  $p\pi^-$  distribution. However, the  $\pi^-p$  distribution is less accurately reproduced in detail than is  $\pi^+p$ , for the large  $s_{\pi N}$ . The graphs of Figs. 11 and 12 have had experiment and theory normalized to the same area, to make comparison of details simpler. Again this is not much of an adjustment, due to the good over-all normalization of the calculation. The relative size of  $p\pi^+$  and  $p\pi^-$  distributions at low  $M_{\pi p}$  is approximated fairly well by the model.

Since our model treats the  $\pi\pi$  and  $\pi N$  vertices symmetrically, we could equally well use it to investigate nucleon "resonances" similar to the  $A_1$ . A study of this sort<sup>16</sup> would concentrate on a given  $p\pi^+\pi^-$  mass range; we have not undertaken such a study. We can, however, compare our distribution in  $p\pi^+\pi^-$  mass with the experimental events, choosing only those with  $M_{3\pi}$  in the  $A_1$  or the  $A_3$  region. This is done in Fig. 13, where we plot  $M_{p\pi^+\pi^-}$  for the least-forward  $\pi^-$  (choice of the least-forward  $\pi^-$  limits us to  $p\pi^+\pi^-$  combinations which are most likely to be traveling together). Again the qualitative agreement is good. This is encouraging because we were not focusing on  $p\pi^+\pi^-$  systems when we set up the Reggeization formula, and this distribution is essentially a by-product of the calcula-

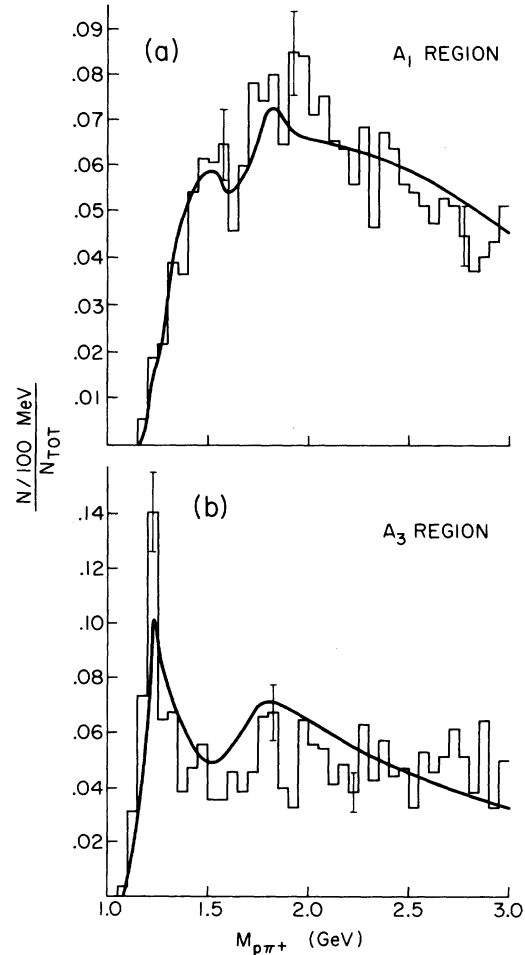


FIG. 11. Distribution in  $M_{p\pi^+}$ : (a) in  $A_1$  region; (b) in  $A_3$  region.

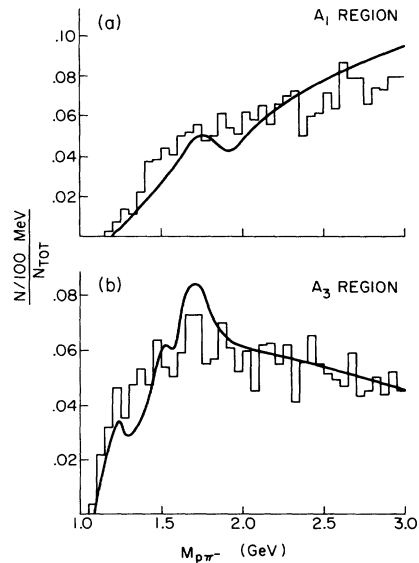


FIG. 12. Distribution in  $M_{p\pi^-}$ : (a) in  $A_1$  region; (b) in  $A_3$  region.

tion. Agreement here tends to support our belief in the validity of the model.

#### IV. PARTIAL WAVES DERIVED FROM EXPERIMENTAL FITTING ROUTINE

The similarity of the various calculated distributions to their counterparts in the data encouraged a hope that the individual partial waves in the three-pion system might also be predicted accurately by the model. Amplitudes and phases of the partial waves in the data were obtained by Ascoli *et al.* using the fitting routine of Ref. 2; we used the same fitting routine on our Monte Carlo-generated sample of events. To have good statistics for the fitting procedure we generated 8000 events in each  $3\pi$  mass bin (100 MeV wide), at 16 GeV/c. Before discussing the results, let us briefly review the assumptions made in performing the fit.

Events are assumed to proceed by the production of a state of spin  $J$  and spin projection  $M$  which then decays into a dipion system of spin  $S$  and a single pion. The dipion and pion are in some relative orbital angular momentum state  $L$ ; allowance is made for various  $L$ 's and  $S$ 's in each state characterized by  $M$ ,  $J$ , and parity. In general, "coherence" is assumed for different decays of a given  $M$ ,  $J$ ,  $P$  state—both decay modes are assumed to come predominantly from the same spin combination at the nucleon-nucleon vertex. This assumption has been tested in the experimental data (see

Ref. 2) and found to be reasonable; its validity in our Deck model is discussed in I, where the amplitudes are displayed.

Various dipion resonances are allowed in the  $\pi^+\pi^-$  mass:  $f^0$ ,  $\rho$ , and  $\epsilon$ . These are approximated by Breit-Wigner forms with widths and masses taken to be  $\Gamma=0.154$  GeV,  $M=1.269$  GeV for the  $f$ ;  $\Gamma=0.135$ ,  $M=0.765$  for the  $\rho$ ; and  $\Gamma=0.400$ ,  $M=0.765$  for the  $\epsilon$ . The over-all amplitude is then symmetrized in the two  $\pi^-$  particles. No  $\pi^-\pi^-$  dipion states are included. All events in the  $\Delta$  region of  $\pi N$  mass are excluded before fitting; this removes most of the complications introduced by  $\pi N$  resonance formation.

The  $J$  values of greatest interest to us in this region of three-pion mass are 0, 1, and 2. Fits to our Monte Carlo events show that the "unnatural parity" sequence  $J^P=0^-, 1^+, 2^-$  dominates this region, with possibly some  $3^+$  needed at the higher values of  $M_{3\pi}$ . In Fig. 14 we display the amounts of these major spin states calculated from the model at 16 GeV/c. These may be compared with the results of fitting the combined 11–25-GeV/c data displayed in Fig. 15. (In Fig. 15 the solid curve is an "eyeball" fit hand-drawn through the model points of Fig. 14.)

We note in particular the following similarities between the calculation and experiment. (These comments apply to the "main" solution plotted. The "alternate" solutions, indicated by arrows, are discussed at the end of this section):

(i)  $M=0$  states are much more heavily populated than  $M \neq 0$  states, in agreement with the data (not shown).

(ii) The  $1^+ s$  wave has a peak in it near  $M_{3\pi}=1.1$  GeV; there is no peak in the  $1^+ p$  wave  $\epsilon\pi$  at this position and the  $\epsilon\pi$  is considerably smaller than the  $\rho\pi$  at the peak.

(iii) The  $1^+ \epsilon\pi p$  wave rises to meet and cross the  $1^+ \rho\pi s$  wave at larger  $3\pi$  mass.

(iv) The  $0^- p(\rho\pi)$ ,  $1^+ p(\epsilon\pi)$ ,  $2^- p(\rho\pi)$ ,  $3^+$  total, and flat magnitudes are reproduced quite well in shape and size.

(v) The over-all  $2^-$  contribution rises from threshold to a plateau at large values of  $M_{3\pi}$ .

(vi) Outside of the  $A_3$  region, our  $2^- s(f\pi)$  wave is about the right size.

We also note the following differences:

(i) The model predicts too much  $0^-$  compared with  $1^+$ .

(ii) The peak in the  $1^+$  distribution calculated from the model is not as sharp as the peak in the data.

(iii) The  $A_3$  peak does not show at all the Deck-model  $2^- s(f\pi)$  wave.

In summary, all the properties of the  $1^+$  state seem to be predicted approximately correctly, al-

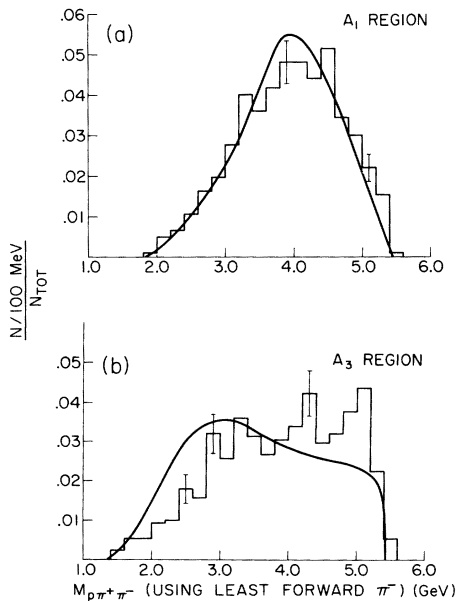


FIG. 13. Distributions in  $M_{p\pi^+\pi^-}$  for the  $\pi^-$  that is least forward from the incident beam: (a) in  $A_1$  region; (b) in  $A_3$  region. Experimental points are from the data of the ABBCH collaboration at 16 GeV/c (Ref. 2).

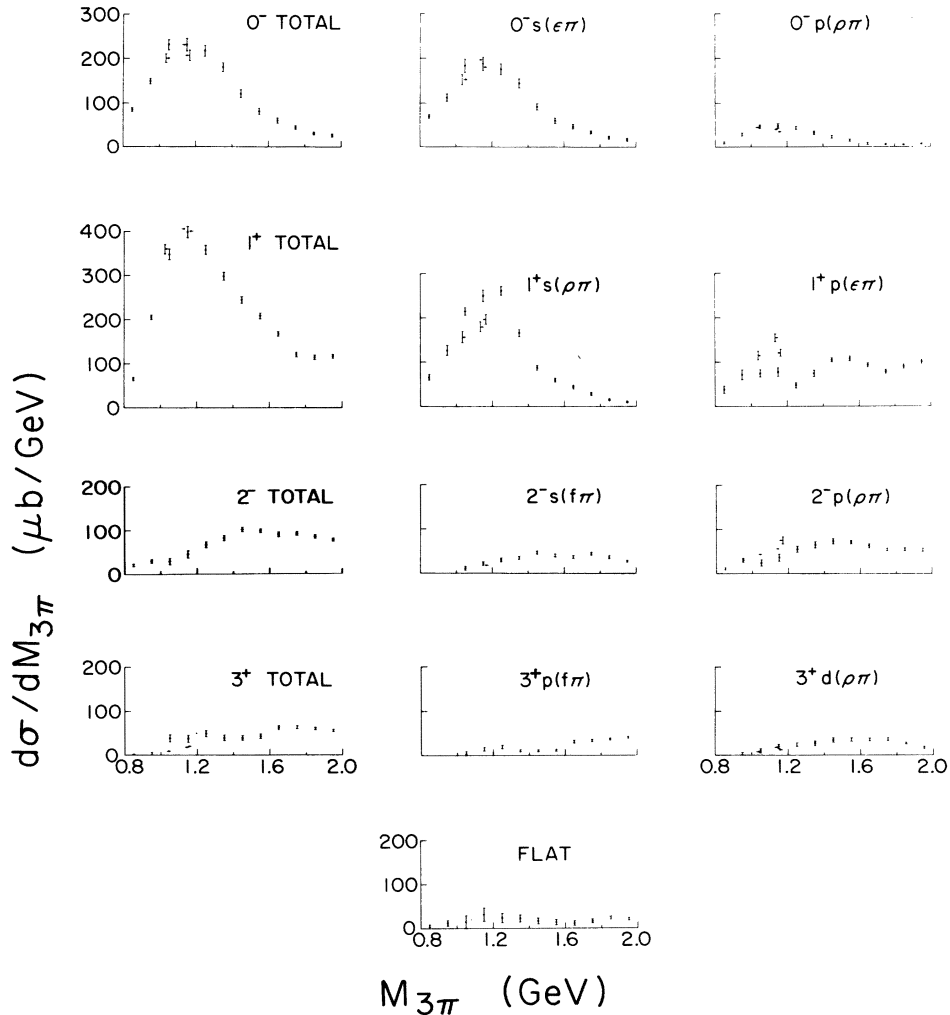


FIG. 14. Magnitude of partial waves obtained by applying FIT to the Deck model.

though exact details are not reproduced. The general shapes of the other partial waves plotted are also correct (except for the  $2^-f\pi$   $s$  wave), but the ratios of sizes may be off as much as a factor of 2 (i.e., 1.4 in the amplitude). Since we have taken an extremely simple model, with no off-shell extrapolation for  $\pi\pi$  and  $\pi N$  partial waves, we feel this is quite good agreement. Possible alterations in the model to change the relative sizes of partial waves are discussed in Sec. VI.

It is important to note that in the study of I, where FIT was tested and compared with explicitly calculated partial waves in a somewhat simpler model, FIT obtained a more rounded  $A_1$  peak than the explicit calculation. Some (but by no means all) of the discrepancy between the  $1^+s$  magnitudes calculated by FIT from the data and from the Deck model may be ascribed to the difficulty FIT has in differentiating between the  $1^+s(\rho\pi)$  and  $1^+p(\epsilon\pi)$

states at low  $3\pi$  mass.<sup>19</sup> However, the fitting program has much more trouble with the Deck model than it did with the data. At the end of this section we discuss this problem in more detail.

Our explicit calculation in I yielded a large  $0^-s(\epsilon\pi)$  wave, like that derived here. We conclude that the model discussed here does in fact produce too much  $0^-s(\epsilon\pi)$ .

Our failure to produce a well-defined  $A_3$  is, however, a disappointment. It is linked closely with the fact that the  $f$  meson is barely visible in our calculated  $\pi^+\pi^-$  distribution. Since SMU gives a slightly better  $f$  than other choices of the pion propagator, we have been unable to improve the situation by varying any of the inputs within our simple framework. The presence of the  $A_3$  is much more obvious in the analytic partial-wave analysis performed in I, which can pick out any partial wave present without regard to its relative

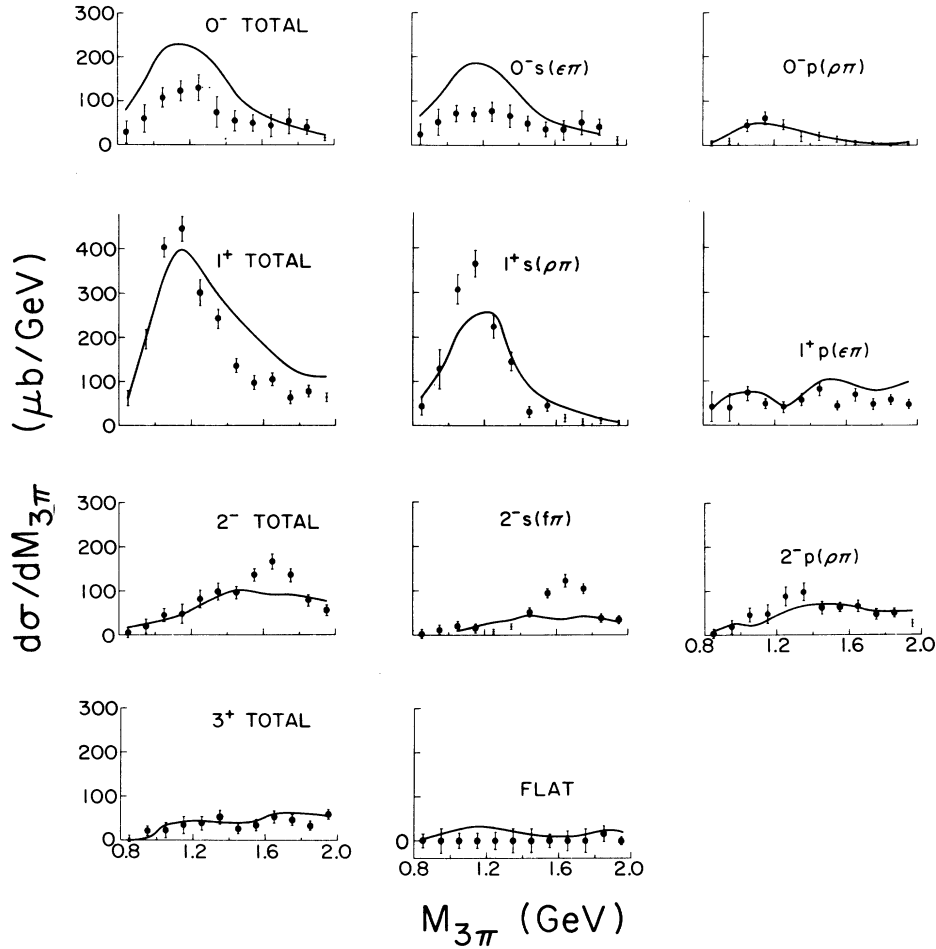


FIG. 15. Magnitude of partial waves obtained by applying FIT to the data. Curves are drawn by hand through the Deck-model points of Fig. 14.

size.

FIT also determines relative phases between different production amplitudes. As mentioned in the Introduction, one of the mysteries associated with the  $A_1$  is the lack of variation of the phase of the  $\rho\pi$   $s$ -wave amplitude relative to other amplitudes present. An associated mystery is the numerical value of the relative phase  $\varphi_{\rho\pi}^{1^+} - \varphi_{\epsilon\pi}^{1^+} \approx 90^\circ$  for  $0.9 \text{ GeV} \leq M_{3\pi} \leq 1 \text{ GeV}$ .<sup>1,20</sup> We therefore wish to examine the predictions of the model for these relative phases.

In Fig. 16 we display the fitted values of relative phases between all the important states from our model, at  $16 \text{ GeV}/c$ . Error bars on the points indicate the statistical accuracy in fitting a finite number of events. The comparable experimental phases are shown in Fig. 17. We see that on the whole the approximate magnitudes of the phases are given reasonably well by the model. We feel this indicates that a Deck-type model can come

close to describing all the measurable physical quantities of the three-pion system in the  $A_1$  region. Approximate agreement of the phases in the  $A_3$  region is probably fortuitous, as the small magnitude ascribed by FIT to our  $2^-s(f\pi)$  wave precludes trust in the phases obtained for this wave. In a maximum-likelihood fit with a finite number of states in the hypothesis, small states tend to act as "garbage collectors," picking up all those contributions which fail to resemble the large states assumed. For this reason, the peculiar fluctuations seen in some of the  $2^-$  phases in Fig. 16 are not surprising, considering the small  $2^-s(f\pi)$  magnitude shown in Fig. 14.

At first glance the  $90^\circ$  phase difference between production of  $1^+p$ -wave  $\epsilon\pi$  and  $1^+s$ -wave  $\rho\pi$  seems strange. One might wonder whether this result could be easily understood. We have studied this particular phase in the region  $1.0 \text{ GeV} \leq M_{3\pi} \leq 1.1 \text{ GeV}$  by generating events according to a series of

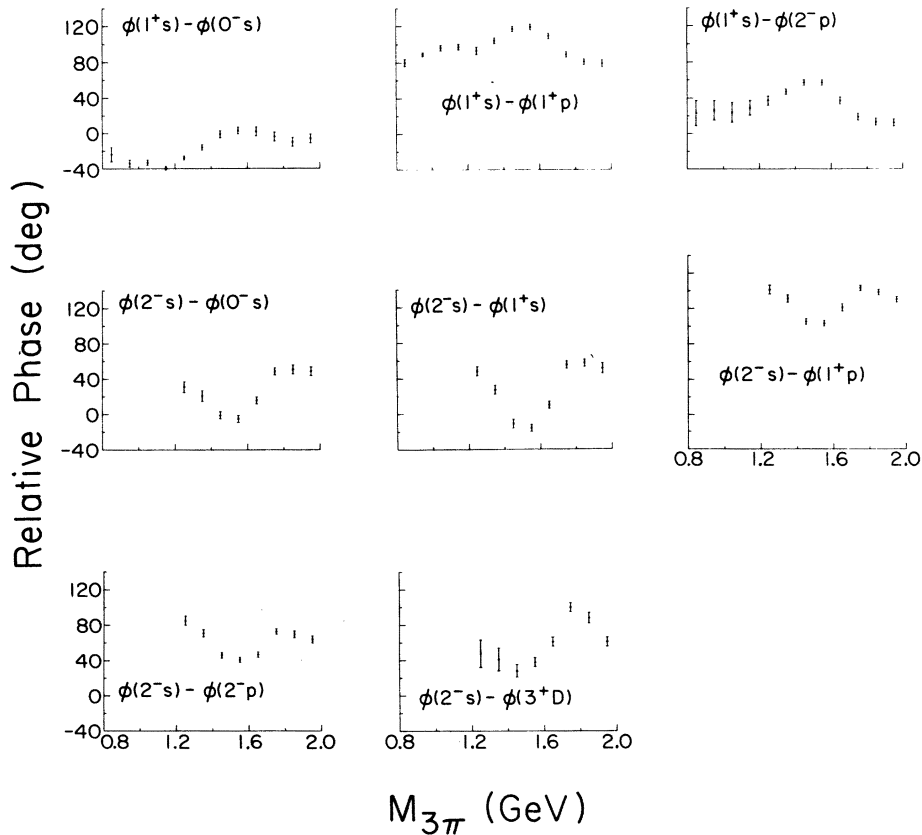


FIG. 16. Relative phases between partial-wave amplitudes obtained by applying FIT to the Deck model.

models and fitting them; within the Deck framework this phase difference is due almost entirely to the Regge signature factor of the pion exchange.

Let us begin with the simplest possible version of our model—set the  $\pi^-\pi^-$  scattering amplitude equal to zero, replace the  $\pi^+\pi^-$  scattering amplitude by Breit-Wigner forms at common  $\rho$ - $\epsilon$  mass, replace the  $\pi N$  scattering by a pure Pomeron exchange, and put in a pion propagator with no signature (for example a non-Reggeized elementary pion). Clearly the  $1^+s$ -wave  $\rho\pi$  and  $1^+p$ -wave  $\epsilon\pi$  states produced by this must be relatively real. We fitted events generated from this model, and indeed obtained a relative phase of  $0^\circ$ .

Next, we allowed the full  $\pi^+\pi^-$  scattering amplitude to be present. Some phase difference will be introduced in the fit by the fact that the Protospopescu  $\epsilon$  is not at the pole position of our Breit-Wigner form. Upon fitting these events we found  $\varphi_{1^+s} - \varphi_{1^+p} = 26^\circ$ . The next step was to allow the full  $\pi^+\pi^-$  scattering amplitude along with the full  $\pi N$  scattering (as in PDK with  $a=2$ ). This yielded a relative phase of  $23^\circ$ . Finally we Reggeized the pion propagator as in SMU and allowed it to have signature. The relative phase came back to  $\varphi_{1^+s} - \varphi_{1^+p} \approx 95^\circ$ .

Clearly the Reggeization procedure can make the production phases of  $\epsilon\pi$   $p$  wave and  $\rho\pi$   $s$  wave different. To our knowledge, the study of phases in this model is the first time it has been possible to test, even indirectly, the phase of pion exchange. Our results support the concept of a signature-factor phase with nonzero  $\alpha(t)$  for this exchange.

As mentioned briefly above and as shown in Fig. 14, some problems were encountered in fitting the events generated according to the Deck model. One possible cause of this is discussed in Ref. 19, where we show that the (symmetrized) decay amplitudes for the states  $1^+s(\rho\pi)$  and  $1^+p(\epsilon\pi)$  are rather similar. This leads, in fitting the data, to a rather poor determination of the relative amounts for the two states below  $M_{3\pi} = 1.1$  GeV. There is no corresponding problem in determining the relative phase. In fitting the Deck-model events, this problem turns out to be much more severe. Not only is the effect noticeable to higher  $M_{3\pi}$  (up to  $M_{3\pi} \sim 1.4$  GeV), but in fact (as shown in Fig. 14) two solutions were found in some  $M_{3\pi}$  bins. The two solutions are shown in Fig. 14, distinguished by left and right arrows. It is our impression that this difficulty in applying the fitting program is

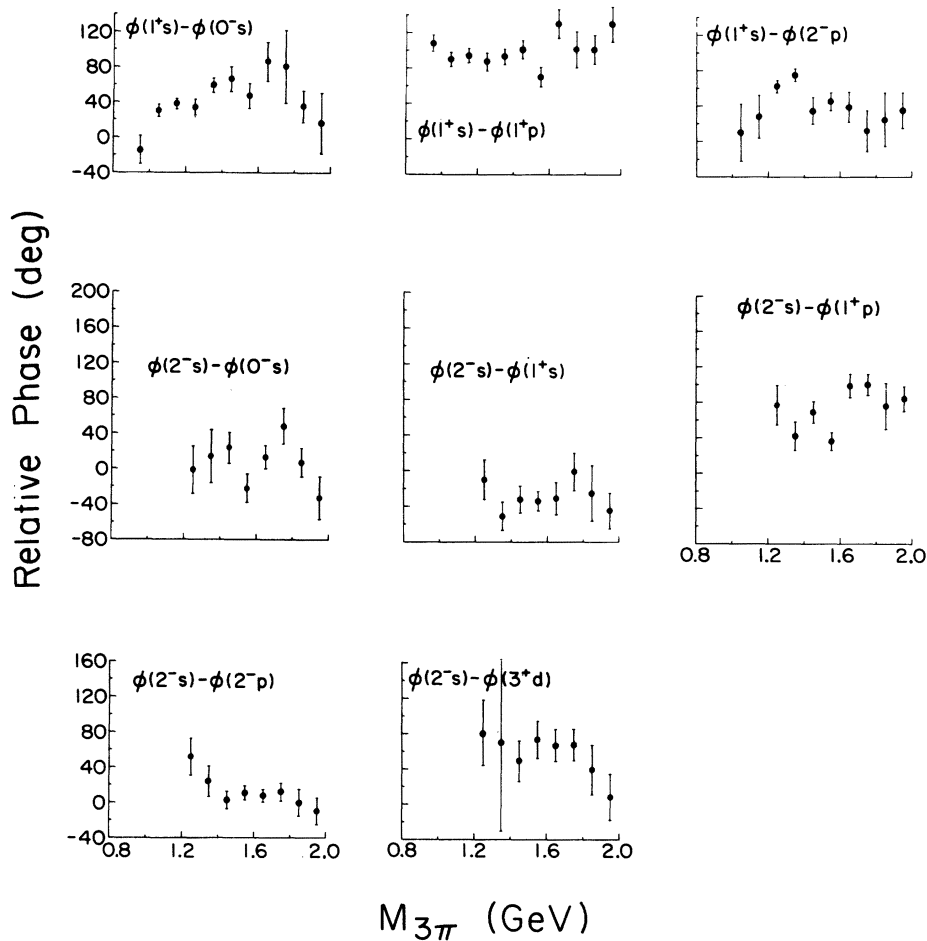


FIG. 17. Relative phases between partial-wave amplitudes obtained by applying FIT to the data.

due to the large amount of  $0^-s(\epsilon\pi)$  present in the model.

Because FIT assumes a sequential decay of the  $3\pi$  states which is not present in the Deck model, it is possible that FIT simply cannot reproduce the Deck model. One test for this is to generate events using the formula FIT has chosen, and to compare these events with the original sample of Deck events. If the fit is truly good, the two sets of events should produce identical histograms in all the kinematic variables. The fit to the data presented in Ref. 2 passed this test with flying colors; it is appropriate to ask whether FIT can do as well for the Deck model. We find that in the  $A_1$  region, FIT closely matches the Deck events. However, some problems show up in the  $A_3$  region.

In Fig. 18 we compare the fit (solid curve) with the Deck events (histogram) at  $1.6 \text{ GeV} \leq M_{3\pi} \leq 1.7 \text{ GeV}$  for the two projections of the  $3\pi$  Dalitz plot. The  $\pi^+\pi^-$  projection is reproduced adequately by FIT, although the  $\rho$  peak is slightly displaced and the low  $\pi^+\pi^-$  mass region is underestimated. How-

ever, the FIT result fails to match the large notch in the Deck  $\pi^-\pi^-$  distribution. Also, it seriously underestimates the  $\cos\beta$  distribution near  $\cos\beta = -1$  (not shown). The azimuthal distributions ( $\alpha$  and  $\gamma$ ) are reproduced reasonably well.

We know that the  $\pi^+\pi^- s$  wave used by FIT is rather different from that in our model, since FIT uses only a Breit-Wigner form at  $765 \text{ MeV}$ , while our “ $\epsilon$ ” effect is rather more complicated. To determine whether this difference was at the heart of our troubles, we refitted the Deck sample using instead of the Breit-Wigner  $\epsilon$  the  $\pi^+\pi^- s$ -wave scattering amplitude actually used in the Deck calculation.<sup>4</sup> The likelihood for this fit was increased by a substantial amount over the “regular” fit. Results are shown as the dashed curves in Fig. 18.

The modified fitting routine reproduces the Dalitz-plot distributions better. It does not help much with the  $\cos\beta$  distribution. Examination of the Dalitz-plot distributions indicates that the “notch” is a feature of  $\rho$ - $\epsilon$  interference, assoc-

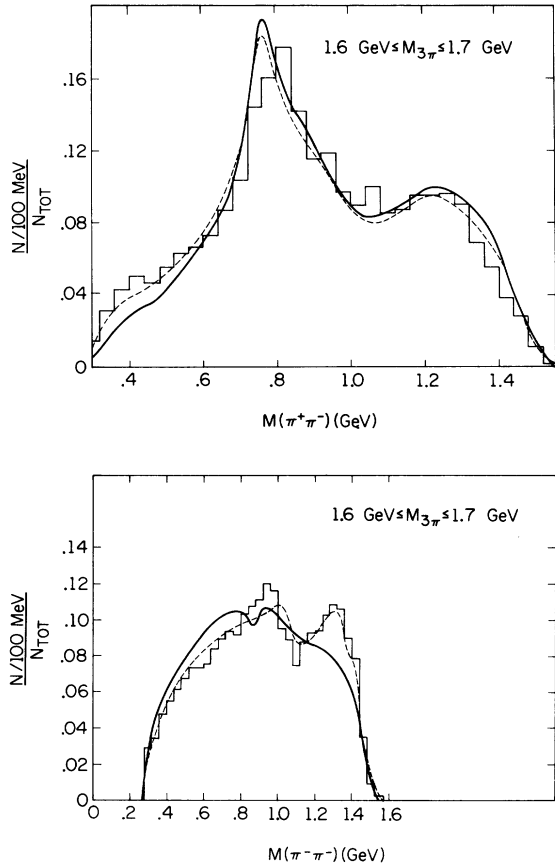


FIG. 18. Comparison of Deck events with events generated from fits to Deck model. The histogram shows original events, the solid curve is generated from the normal fit, and the dashed curve is generated from the fit using the Protopopescu (Ref. 4)  $\pi^+\pi^-$   $s$ -wave amplitude. (a) Projection on  $M_{\pi^+\pi^-}$ ; (b) projection on  $M_{\pi^-\pi^-}$ .

iated with the particular  $\epsilon$  in our model. It is not obviously present in the data.

The parameters of the fit which are most affected by the change in  $s$ -wave form are the relative phases between different states, which change typically by  $\sim 30^\circ$ .

#### V. OTHER CALCULATIONS WITH THE MODEL

Encouraged by our success in the  $A_1$  region, we turned to the reaction  $\pi^-n \rightarrow \pi^- \pi^- \pi^0 p$ , measured by Katz *et al.*<sup>21</sup> at 7 GeV/c. Our model assumes that this reaction proceeds by the mechanism of Fig. 19, which depends on  $\pi N$  charge-exchange scattering at one vertex. Hence calculation of this reaction tests the isospin dependence of our model.

In Fig. 20(a) we present our calculation of the uncut  $3\pi$  spectrum together with the data of Katz *et al.*<sup>21</sup> The agreement is quite good, considering the sort of normalization problems which may

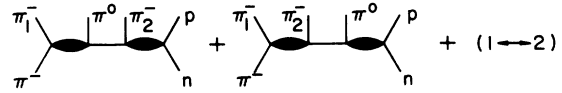


FIG. 19. Our Deck model for  $\pi^-n \rightarrow \pi^- \pi^- \pi^0 p$ .

arise in extracting neutron cross sections from the experiment on deuterium. Note that no  $A_1$ -like peak is present in the over-all  $3\pi$  spectrum.

Cohen *et al.*<sup>22</sup> have shown that if various cuts are made on this spectrum an  $A_1$ -like peak may be produced in the doubly charged meson system. We imposed these cuts on our generated events and obtained the curve shown in Fig. 20(b). We see that a peak is obtained and the agreement with the data of Cohen *et al.* is again quite reasonable. [In Fig. 20(a) and 20(b) we present our calculation as a histogram with errors attached because only a small sample of Monte Carlo events was generated for this reaction. For  $\pi^-p \rightarrow \pi^- \pi^+ \pi^- p$ , on the other hand, a large number of events was generated and we feel justified in drawing the smooth curves presented above.]

If we believe that the Pomeron trajectory used by Barger and Phillips in their parameterization of  $\pi N$  scattering is correct, we may use the model to calculate  $A_1$  production at any arbitrary energy desired. Anticipating NAL energies, we have calculated the cross section for the process  $\pi^-p \rightarrow \pi^- \pi^+ \pi^- p$  in the region  $1.05 \text{ GeV} \leq m_{3\pi} \leq 1.25 \text{ GeV}$  for momenta up to  $p_{\text{lab}} = 640 \text{ GeV}/c$ . The results are displayed in Fig. 21. We see that the cross section is expected to decrease slowly with increasing energy, with the result at 640 GeV/c about half of that at 20 GeV/c. This is similar to the  $1/\ln s$  decrease expected of any Regge model

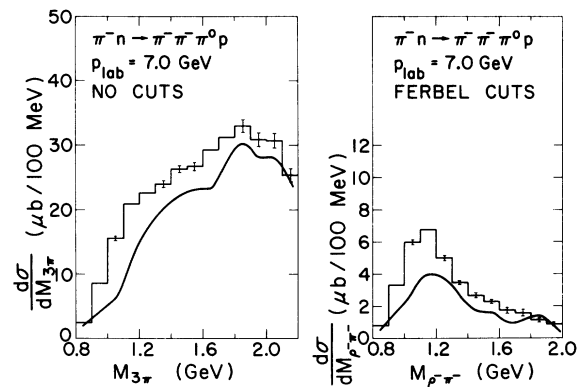


FIG. 20. (a) The  $3\pi$  mass in  $\pi^-n \rightarrow \pi^- \pi^- \pi^0 p$ . Curve is drawn by hand through data from Ref. 21; histogram is prediction of our model. (b) The  $\rho^-\pi^-$  mass spectrum in  $\pi^-n \rightarrow \pi^- \pi^- \pi^0 p$  after Ferbel cuts ( $|t_{\rho-\pi^-}| < 0.5 \text{ GeV}^2$ ,  $M_{\rho\pi^-} > 1.5 \text{ GeV}$ ) were made. The curve is drawn by hand through data from Ref. 22; histogram is the prediction of our model.

integrated over  $t$ ; however, the decrease cannot be parametrized exactly by  $1/(a \ln s + b)$ . This is probably because the integration over  $s_{\pi N}$  slightly smears out the behavior anticipated from the Regge contribution to high-energy  $\pi N$  scattering.

#### IV. CONCLUSIONS AND DISCUSSION

We conclude that the Reggeized Deck model agrees qualitatively with the data for  $\pi N \rightarrow 3\pi N$  in the  $A_1$  region of  $3\pi$  mass, and that in many respects the agreement is quantitative as well. Individual partial waves in this region are predicted accurately to within a factor of 2 in intensity, which is quite good for a strong-interaction calculation. The over-all normalization of the sum of partial waves is also quite close to that of the data. One particular feature of agreement, the  $90^\circ$  phase difference between the  $1^+ s$  and  $1^+ p$  waves, stems directly from the signature phase of the exchanged Reggeized pion. To our knowledge, this is the only experimental test to date of the phase of pion exchange, and we view the agreement as striking confirmation of the Regge model.

The agreement of all  $3\pi$  angular distributions in the low  $M_{3\pi}$  region shows that the polarization of the produced  $A_1$  is correctly predicted. This is known experimentally to be  $t$ -channel helicity  $0^{23}$ ; we show it theoretically in I.

Other details are not reproduced as well. Relative to the  $1^+ \rho\pi$  s wave, the calculated  $0^- \epsilon\pi$  s wave is too large and the calculated  $2^- f\pi$  s wave is too small. Hence, the  $A_3$  effect is obscured by  $\rho\pi$  and  $\epsilon\pi$  partial waves. As discussed in the Introduction,

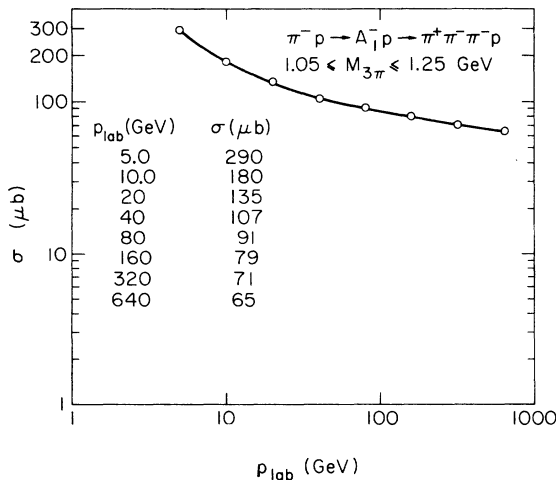


FIG. 21. Prediction of the Deck model for high-energy production of the  $A_1$  bump.

this could no doubt be improved by making an off-mass-shell extrapolation of the  $\pi\pi$  and  $\pi N$  scattering amplitudes.

We have experimented with a few of the many possible changes which could be made in the model, to see whether they would lead to a reduction in the  $0^- \epsilon\pi$  s wave and an increase in the  $2^- f\pi$  s wave. One possibility is to use the sort of form factors advocated by Wolf<sup>24</sup> in his study of  $\pi$  exchange. Insertion of these form factors (functions of the momentum of the exchanged Reggeon and the masses at the  $3\pi$  vertex) does lead to a reduction in the  $0^- \epsilon\pi$  s wave; however, we were unable to increase the  $2^- f\pi$  s wave within this framework even if we manipulated the "radius" parameter for this wave.

Another possible modification of the amplitude can be achieved by noting that for large  $s_{12}, s_{23}$  in Fig. 4,  $s_{23} \sim s_{123}/s_{12}$ . Hence for large  $s_{12}, s_{23}$  we should have  $(s_{123}/s_{12})^{\alpha_\pi} = (s_{123}/s_0)^{\alpha_\pi} (s_0/s_{12})^{\alpha_\pi}$  rather than  $(s_{123}/s_0)^{\alpha_\pi}$  [and similarly if  $s_{123}$  is replaced by  $\frac{1}{2}(S_{3\pi} - U_{3\pi})$ ]. Thus for large  $s_{12}$  and  $s_{23}$  our amplitude should be multiplied by  $(s_{12}/s_0)^{|\alpha_\pi(t_R)|}$ . We do not have such large values of  $s_{12}$  and  $s_{23}$ , but perhaps a factor of this sort might help. To avoid letting the factor get too small for small  $s_{12}$ , we tried an *ad hoc* correction factor of  $[(s_{12} + 0.5)/s_0]^{|\alpha_\pi(t_R)|}$ . This did reduce the  $0^- \epsilon\pi$  s wave a bit and increase the  $2^- f\pi$  s wave by almost a factor of 2 in (magnitude)<sup>2</sup>, while leaving the  $\rho\pi$  waves more or less unchanged.

We see, therefore, that it should be possible by a series of small adjustments in the model to reproduce the  $A_3$  region as well as the  $A_1$  region. The adjustments explored above can be rationalized fairly easily, although such rationalizations and adjustments are more of an art than a science at present.

Previous discussions of the reaction<sup>25</sup>  $\pi^- p \rightarrow \pi^- \rho^0 p$  have emphasized the necessity of adding the graph shown in Fig. 22(a) to that shown in Fig. 3. While we do not have this contribution explicitly, we do have the contribution shown in Fig. 22(b). At low  $s_{23}$  this has no resonances; however, it might be expected to approximate the *average* of



FIG. 22. The amplitude represented by diagram (a) is not found explicitly in our model, but the model does contain  $\rho$  exchange, as shown in (b). The Reggeized pion propagator of (b) should contain some average over produced 23 resonances. Hence we do not add terms like (a).

such resonances in the usual sense of duality. We therefore feel that the bulk of Fig. 22(a) has been taken into account. This agrees with the fact that our predicted magnitudes are much closer to those

of the data than is customarily found using the diagram of Fig. 3 alone.

Spin structure of the amplitude at the nucleon vertex is discussed in I.

†Work supported in part by the U. S. Atomic Energy Commission under Contract No. AT(11-1)-1195.

‡Work supported in part by NSF under Grant No. NSF GP25303.

<sup>1</sup>D. Brockway, thesis, Univ. of Illinois Report No. COO-1195-197, 1970 (unpublished); Y. M. Antipov *et al.*, in *Experimental Meson Spectroscopy—1972*, proceedings of the third international conference on experimental meson spectroscopy, Philadelphia, 1972, edited by Kwan-Wu Lai and Arthur H. Rosenfeld (A.I.P., New York, 1972), p. 164; G. Ascoli, in *Proceedings of the XVI International Conference on High Energy Physics, Chicago-Batavia, Ill., 1972*, edited by J. D. Jackson and A. Roberts (NAL, Batavia, Ill., 1973), Vol. 1, p. 3; Y. M. Antipov *et al.*, submitted to the second Aix-en-Provence Conference, 1973 (unpublished).

<sup>2</sup>Illinois-GHMS-H-ABBCCH-ND-W and CIBS Collaborations, in *Experimental Meson Spectroscopy—1972* (Ref. 1), p. 185; G. Ascoli *et al.*, *Phys. Rev. D* 7, 669 (1973); Y. M. Antipov *et al.*, submitted to the second Aix-en-Provence Conference, 1973 (unpublished).

<sup>3</sup>E. L. Berger, *Phys. Rev.* 166, 1525 (1968).

<sup>4</sup>S. D. Protopopescu *et al.*, *Phys. Rev. D* 7, 1269 (1973).

<sup>5</sup>J. P. Baton, G. Laurens, and J. Reignier, *Phys. Lett.* 33B, 528 (1970).

<sup>6</sup>W. D. Walker *et al.*, *Phys. Rev. Lett.* 18, 630 (1967).

<sup>7</sup>C. Lovelace, R. M. Heinz, and A. Donnachie, *Phys. Lett.* 22, 332 (1966).

<sup>8</sup>J. H. Scharenguivel *et al.*, *Nucl. Phys.* B22, 16 (1970).

<sup>9</sup>B. Y. Oh *et al.*, *Phys. Rev. D* 1, 2494 (1970).

<sup>10</sup>P. Estabrooks *et al.*, CERN Report No. Th. 1661 (unpublished).

<sup>11</sup>A. Donnachie, R. G. Kirsopp, and C. Lovelace, *Phys.*

*Lett.* 26B, 161 (1968). We used the CERN theoretical (1967) phase shifts obtained from a tape kindly provided to us by the Particle Data Group.

<sup>12</sup>V. Barger and R. J. N. Phillips, *Phys. Rev.* 187, 2210 (1969).

<sup>13</sup>G. Ascoli *et al.*, *Phys. Rev. D* 8, 3894 (1973). Hereafter we will refer to this as I.

<sup>14</sup>R. T. Deck, *Phys. Rev. Lett.* 13, 169 (1964).

<sup>15</sup>S. D. Ellis and A. I. Sanda, *Phys. Rev. D* 6, 1347 (1972).

<sup>16</sup>S. T. Jones, *Phys. Rev. D* 2, 856 (1970).

<sup>17</sup>All data used for comparison in this paper were taken from the compilation made by Ascoli and Kruse at the University of Illinois for the purpose of studying the  $A_3$  effect. Particular groups of contributors are listed in Ref. 2.

<sup>18</sup>We remark in passing that a calculation of the Berger type for  $\pi^-p \rightarrow \pi^- \pi^0 p$  leads to a similarly disappointing result for the  $A_3$ , in that the ratio of the predicted  $A_3$  peak to the  $A_1(\rho\pi)$  peak is smaller than in the data.

<sup>19</sup>B. Weinstein, G. Ascoli, and L. M. Jones, *Phys. Rev. D* 8, 2904 (1973).

<sup>20</sup>In comparing our phases to those reported by Ascoli *et al.* in Refs. 1 and 2, a slight adjustment must be made. Our phases are those which one would calculate from the analytic partial-wave amplitudes derived in I. These amplitudes differ by a factor  $(-1)^S$  from those used by Ascoli *et al.* in previous work, where  $S$  is the spin of the dipton system. This arises from a difference in definition of the  $\pi\pi$  scattering angle.

<sup>21</sup>W. Katz *et al.*, *Phys. Lett.* 31B, 329 (1970).

<sup>22</sup>D. Cohen *et al.*, *Phys. Rev. Lett.* 28, 1601 (1972).

<sup>23</sup>G. Ascoli *et al.*, *Phys. Rev. Lett.* 26, 929 (1971).

<sup>24</sup>G. Wolf, *Phys. Rev.* 182, 1538 (1966).

<sup>25</sup>L. Stodolsky, *Phys. Rev. Lett.* 18, 973 (1967).